

JBBM 00854

A new method for the determination of the permittivity of small samples in the microwave range and its application to hemoglobin single crystals

W. Daseler, H.-J. Steinhoff and A. Redhardt
Institut für Biophysik, Ruhr-Universität Bochum, Bochum, F.R.G.

(Received 11 May 1990)

(Accepted 6 August 1990)

Summary

A cavity perturbation method for the absolute determination of the complex permittivity of small samples in the microwave range is developed and tested. Samples with volumes less than 0.4 mm^3 , for example protein powder or single crystals of macromolecules, may be investigated in a temperature range between 180 and 300 K, using this method. As an application the complex permittivity of hemoglobin single crystals is determined at three frequencies, $\nu = 3.06 \text{ GHz}$, $\nu = 8.76 \text{ GHz}$ and $\nu = 17.0 \text{ GHz}$ in a temperature range between 180 and 300 K.

Key words: Permittivity; Protein crystal; Hemoglobin

Introduction

The dielectric properties of macromolecules are essentially determined by the mobility of polar amino acid residues at the molecules surface and by the mobility of water molecules in the hydration shell(s), which are adjacent to the macromolecule. The mobility of these components at the surface of the protein has been investigated in solution by EPR, NMR and by dielectric methods [1–4].

These mobile surface parts seem to play an important role in biochemical reaction mechanisms, as shown in recent investigation (see for example Ref. 5 and literature therein). However, recent molecular dynamics calculations [6] are in

Correspondence address: H.-J. Steinhoff, Institut für Biophysik, Ruhr-Universität Bochum, Postfach 102148, D-4630 Bochum 1, F.R.G.

partial contradiction to the results [2–4] concerning the role of bound water in surface phenomena observed there.

Therefore, new information to these basic results [1–4] on macromolecules, using modern experimental and numerical techniques seems to be of interest. Especially, the investigation of single crystals should be of outstanding interest, because the surface geometry of the molecules is well known by X-ray crystallography and computer graphics. Additionally, the packing density of the macromolecules in single crystals is high. This results for example in high values of the surface water part to the intermolecular water part, facilitating the discrimination between volume and surface effects. It should be stressed that the volume part of water in these crystals (up to 53%) is high enough to give the results biochemical relevance. A method, which is concerned with dielectric molecular surface phenomena in single crystals seems to be important in this conflicting situation.

Because of the smallness of macromolecular crystals ($\leq 0.4 \text{ mm}^3$) only resonant methods such as the cavity perturbation techniques [8–10] can be applied. The method introduced here has the following advantages:

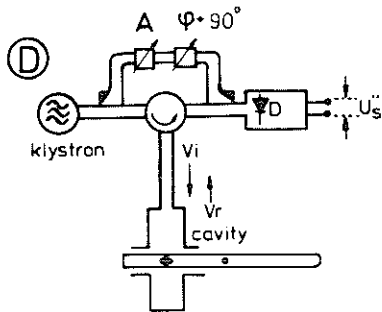
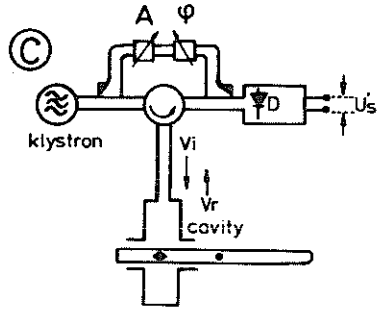
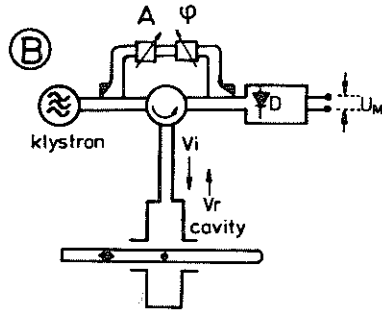
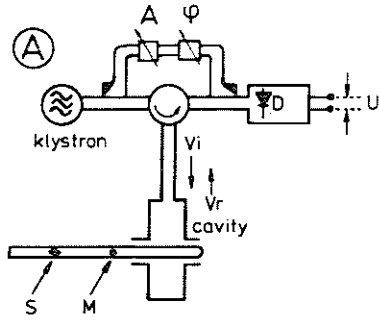
1. The field distribution in the microwave cavity used does not need to be calculated. Therefore, the sample geometry can be optimized with respect to experimental criteria. For example, quartz dewars can be used for low temperature measurements.
2. The typical methods [8–10] cited above use alternatively the determination of cavity quality factors, filling factors or the dielectric constant of a calibration sample, power reflection coefficients and coupling factors. This is not necessary here.

The method presented here is based on a first-order perturbation theory, uses a low Q cavity, and small complex voltage reflection coefficients. The physical idea has been introduced and applied in a preceding paper [7] for the determination of radical concentrations.

Principle of the method

In this section we will give a summary of the principle of the method. The sample under test is placed into the electric field inside a microwave cavity. The polarization of the sample depends on its shape and orientation in the field and can be calculated in closed form only for ellipsoids of revolution [11]. Sample shapes of

Fig. 1. Microwave voltage generated by a klystron is fed to the cavity (voltage amplitude of the incident power, V_i). A quartz tube containing the sample S and a reference metal sphere M can be shifted inside the cavity. The microwave voltage, V_r , reflected from the cavity and containing the information about the dielectric sample properties is monitored by an exact linear detector D /amplifier system. Additionally this system is phase sensitive against the phase of V_r . Practically, this linearity and phase sensitivity is achieved by generating a large microwave bias of the detector D by means of a branch line with variable attenuator A and variable phase shifter, ρ . The figure parts A to D illustrate the different steps of the calibration and the measurement. For details see text.



special experimental interest (for example capillary tubes filled with the substance under test, thin needle-like samples or thin sheets) can be accounted for by the limits of the axis ratios of the ellipsoids: rod-shaped samples and samples with the shape of thin plates are approximated by ellipsoids with axis ratios $\gg 1$ and $\ll 1$, respectively. The equations given here are valid for samples of these shapes situated with their long axis parallel to the electric field. The derivations of these equations as well as further criteria for the validity will be given in the next section.

Fig. 1 sketches the apparatus and the different calibrations during the measurement. Microwave power generated by a klystron passes a circulator and is fed into a cavity. A quartz tube containing the sample under test and a small reference metal sphere can be shifted inside this cavity in a reproducible way. To determine the permittivity of the sample, four different measurements are necessary.

Tuning and matching of the cavity (cf. Fig. 1A)

In the starting position, there are no sample and no reference sphere inside the cavity. The cavity is tuned and matched by a proper choice of the matching iris. No reflected voltage, V_r , exists, and the output voltage, U , of the receiver is $U = 0$.

Calibration (cf. Fig. 1B)

Decreasing the attenuation of the variable attenuator, A , the receiver diode is biased. Now the sample holder is shifted in such a way that the reference metal sphere is inside the cavity. This cavity perturbation produces a reflected microwave voltage, V_r . By means of the phase shifter, ρ , the phase of the bias is changed in a way that the reflected voltage, V_r , leads to a maximum change of the dc output of the receiver. This voltage change is called U_M and is related to the incident microwave voltage, V_i , the filling factor of the metal sphere, η_M , and the quality factor, Q_0 of the empty cavity by:

$$U_M = 3/2kV_i\eta_M Q_0. \quad (1a)$$

where k is a conversion constant.

Determination of ϵ' of the sample (cf. Fig. 1C)

Now the sample holder is shifted again and the sample with filling factor η_s is inside the cavity. The dc-output change of the receiver is given by:

$$U_s' = 1/2kV_i\eta_s Q(\epsilon' - 1) \quad (1b)$$

Determination of the dielectric loss ϵ'' of the sample (cf. Fig. 1D)

The bias phase is changed by 90° compared to its former value. This change in the bias phase of the diode makes the apparatus now sensitive for ϵ'' . A dc-output change U_s'' results:

$$U_s'' = 1/2kV_i\eta_s Q\epsilon'' \quad (1c)$$

Dividing Eqn. 1b by 1a and Eqn. 1c by 1a, and setting $Q \approx Q_0$, we get the final formulae for the determination of ϵ^* of the sample:

$$\epsilon'' = 3U_s'' \cdot v_M / (U_M \cdot v_s) \quad (2a)$$

$$(\epsilon' - 1) = 3U_s' \cdot v_M / (U_M \cdot v_s) \quad (2b)$$

v_s and v_M are the volumes of the sample and the metal sphere, respectively. The simple Eqns. 2 hold, if the following conditions are fulfilled:

The size, shape and orientation of the sample in the cavity must be chosen in a way that the electric field inside the whole cavity is not changed when the sample is inserted (perturbation condition). The perturbation has to be small so that the reflected microwave voltage, V_r , is small compared to V_i , and the cavity quality factor, Q , of the cavity with sample is approximately equal to Q_0 . The dc-voltage, U , must be proportional to the microwave reflected voltage, V_r , for the linear Eqns. 1a–1c to be correct. The remaining settings of the apparatus (except microwave phase, ρ) must be constant in the measurements A–D throughout. Then the constant k in every Eqn. 1a–1c has the same values in these measurements and cancels, as does Q_0 . It should be stressed, that the simple Eqns. 2 do not contain amplifier and crystal characteristics expressed in k , as well as power levels (V_i) and cavity quality factors Q . Also no assumptions were made concerning the field distribution in the cavity.

These restrictions are necessary, however, in the known perturbation techniques [9,10], limiting the accuracy of those methods.

Theory

Derivation of the relations 2

Energy considerations. We start with general relations, which are independent of special cavity shapes. The cavity quality factor Q_0 of the empty cavity is defined as

$$Q_0 = \omega W / P \quad (3)$$

W is the time average of the energy stored in the cavity at resonance, P the power loss per cycle in the cavity, and ω the angular frequency.

The field energy contained in the empty volume v_s , which is occupied later on by the sample, is given by $1/2 \epsilon_0 E_0^2 v_s$, using the above perturbation condition. E_0 is the maximum value of the electric field inside the (empty) volume v_s . Herewith we define the filling factor η_s of the sample:

$$\eta_s = 1/2 \epsilon_0 E_0^2 v_s / W \quad (4)$$

The filling factor η_M of the metal sphere is defined in a similar manner. To take into account the properties of the dielectric sample, we introduce the value ΔW_s ,

which results as the change of the electromagnetic energy when the sample is shifted from outside the cavity to the measuring position (Fig. 1A and D). Following [11], ΔW_s is connected to the complex permittivity $\epsilon^* = \epsilon' - i\epsilon''$ of the sample in first-order perturbation theory:

$$\Delta W_s = 1/2 \epsilon_0 \cdot E_0^2 \cdot v_s \cdot (\epsilon^* - 1) \quad (5)$$

Combining Eqns. 3, 4 and 5 we get independent of the cavity shape

$$Q \cdot \eta_s \cdot (\epsilon^* - 1) = \omega \Delta W_s / P \equiv \Delta P_s / P \quad (6)$$

Where ΔP_s means the (complex) power change due to the sample. For the metal sphere we obtain:

$$\Delta W_M = 3/2 \epsilon_0 E_0^2 v_M \quad (7)$$

$$3 Q \eta_M = \omega \Delta W_M / P \equiv \Delta P_M / P \quad (8)$$

Equivalent circuit. An arbitrary cavity can be described near an unique resonance by a lumped circuit, c.f. Fig. 2. The resonance frequency, ω_0 , of the cavity is by analogy $\omega_0^2 = 1/(L \cdot C)$; the power loss in the cavity is $P = V^2 \cdot G$, G being real. The additional power due to the sample is given by $\Delta P_s = V^2 \cdot \Delta G^*$, where ΔG^* is

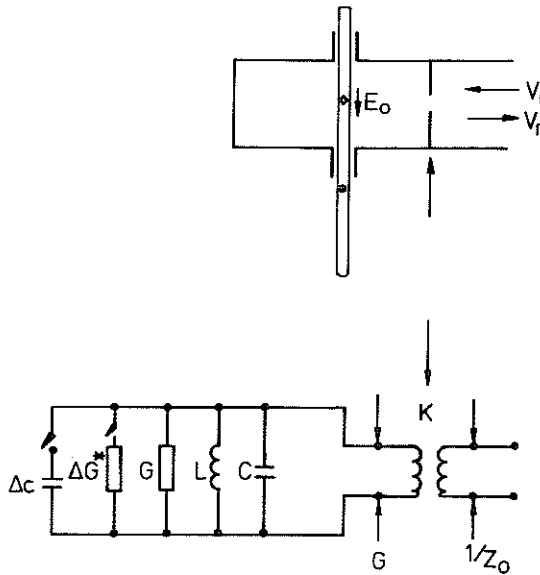


Fig. 2. Reflection type cavity (a) and equivalent circuit (b). The matching iris of the cavity is described by an ideal transformer, matching transforming ratio $K = (Z_0 \cdot G)^{-1}$. Sample and reference sphere are represented by ΔG^* , respectively, ΔC , which can be switched on alternatively.

here the complex according to Eqn. 6. The matching iris of the cavity is described by an ideal transformer, as indicated by the transforming ratio K . Now we assume, that the cavity is tuned ($\omega_{\text{generator}} = \omega_0$). Furthermore, we assume, that the transforming ratio, K , is adjusted in a way, that the (real) wave impedance, Z_0 , of the waveguide appears at the input terminals of the transformer. Then $1/Z_0 = K \cdot G$ holds and the voltage reflection coefficient

$$\rho = \frac{V_r}{V_i} = \frac{1 - Z_0 \cdot K \cdot G}{1 + Z_0 \cdot K \cdot G} \quad (9)$$

is zero for the case A, Fig. 1.

Now, the insertion of the sample (Fig. 1C and D) is accounted for by switching on an additional complex conductance ΔG^* . If

$$\frac{|\Delta G^*|}{G} \ll 1 \quad (10)$$

holds, then Eqn. 9 can be developed, leading in first order to

$$-\rho = -\frac{V_r}{V_i} = \frac{\Delta G^*}{2G} \quad (11)$$

indicating, that the sample causes a complex voltage reflection coefficient ρ . This result is, as the one in Eqns. 6 and 8 independent of the special shape of the cavity.

Combining energy considerations and equivalent circuit

If the equivalent circuit scheme is combined with the energy considerations, it is not necessary to discuss details of the microwave cavity as additional elements of this circuit as done in [8–10]. If, additionally, an independent measurement (here: metal-sphere) delivers the product $\eta \cdot Q$, then the field distribution in the cavity needs not to be known at all and the cavity may have an arbitrary shape. The combination of these two considerations leads to a simple result, if Eqn. 10 holds, which is typical for all perturbation methods. Combination of Eqs. 11 and 6 yields:

$$-V_r/V_i|_s = 1/2Q \cdot \eta_s \cdot (\epsilon^* - 1) \quad (12)$$

where the index 'S' refers to the sample (c.f. Eqn. 4). In a similar manner we get for the metal sphere:

$$-V_r/V_i|_M = 3/2Q \cdot \eta_M \quad (13)$$

If the measuring system is linear, it holds for the dc-output U

$$\begin{aligned} U_s'' &= -k \cdot V_r|_{\text{real part}} \\ U_s' &= -k \cdot V_r|_{\text{mag part}} \end{aligned} \quad (14)$$

The scaling factor k being equal in both cases, as is discussed later on.

It holds:

$$\begin{aligned} U_s'' &= 1/2k \cdot Q \cdot \eta_s \cdot \epsilon'' \cdot V_i \\ U_s' &= 1/2k \cdot Q \cdot \eta_s \cdot (\epsilon' - 1) \cdot V_i \end{aligned} \quad (15)$$

Eqns. 15 are identical with Eqns. 1b and 1c. For the metal sphere M , we get:

$$U_M = 3/2k \cdot Q \cdot \eta_M \cdot V_i \quad (16)$$

which is identical with Eqn. 1a. Combining Eqns. 15 and 16 and remembering the proportionality $\eta \sim v$, we finally get the relations 2.

Conditions for the applicability of Eqns. 2

The Eqns. 2a and 2b seem to be the simplest possible connection between signals U and the unknown ϵ^* . In contrast to Refs. 8–10 they are independent of power level measurements, Q determinations and interpretations of the equivalent circuit in terms of the field distribution in the cavity. This important advance is now founded. It turns out, that the conditions for the applicability of the Eqns. 2 are in favor of biochemical work: the essential point in these conditions is the smallness of the sample under test.

Electric field inside the sample

The two Eqns. 4 and 5, which are essential to the method, express the assumption, that the electric field inside the sample is not changed by the sample itself. The latter affords, that the sample is rodshaped (or has the shape of a thin sheet) and is oriented parallel to the field E_0 , which persists in the cavity in the absence of the sample at the sample's later position. Furthermore, the thickness of the sample must be so small, that neither dielectric polarisation charges on the small side of the sample rod nor skin effects play any role. The effects should be seen by varying the length/thickness ratio, R , of the sample, which varies (as a preparation consequence) with sample size. In 18 experiments with hemoglobin (Hb) single crystals in the volume range $0.03 < v_s < 0.37 \text{ mm}^3$ and a corresponding variation of the length/thickness ratio $5 < R < 3$ we found no systematic dependence of the measured ϵ^* on crystal volume v_s . Furthermore, the upper limit of the skin depths δ_s was calculated from

$$\delta_s = (2/(\omega\mu_0\sigma))^{1/2} \quad \text{with} \quad \sigma = \epsilon_0\omega_0\epsilon''_{\text{Hb}} \quad (17)$$

using our results for the dielectric loss ϵ''_{Hb} of the single crystals. The results were $\delta_s = 12, 5.1$ and 2.6 mm for 3 GHz, 9 and 17 GHz, respectively, and the skin depth can be regarded as large compared to the crystal thickness ($< 0.2 \text{ mm}$) despite of the high content of mother liquid in the crystals (40 Vol% of $(\text{NH}_4)_2\text{SO}_4$, 2 M). From this we conclude, that Eqns. 4 and 5 are valid in our accuracy range also with the high ϵ^* for macromolecular single crystals.

TABLE 1

Cavity properties

1	2	3	4	5	6	7	8	9	10
Reso- nance type ¹	ν / GHz	Q_0	r_M / mm ²	ν /MHz ³	$\frac{Q - Q_0^4}{Q_0}$	δ^5	V / mm ³ ⁶	ϵ'_{Hb} ⁷	$\frac{\epsilon''_{\text{Hb}} + \sigma}{\epsilon_0 \omega}$ ⁷
E ₀₁₀	3.06	380	0.75	1.0	0.06	0.90	0.43	12.64 ± 0.57	3.94 ± 0.26
H ₁₀₁	8.76	130	0.60	6.5	0.038	1.03	0.24	11.88 ± 0.40	2.30 ± 0.18
H ₁₀₃	17.0	300	0.50	10.5	0.057	1.04	0.21	8.0 ± 0.7	2.30 ± 0.34

¹ Cavity dimensions are shown in Fig. 4.² Radius of standard metal sphere.³ Cavity detuning by standard metal sphere.⁴ Change of Q due to a hemoglobin single crystal with $|\rho| = 0.1$.⁵ $\delta = (\epsilon''/\epsilon' - 1)_{\text{it}}/(\epsilon''/(\epsilon' - 1))_{\text{exp}}$, ϵ^* values measured with a thin water layer.⁶ Volume of a hemoglobin single crystal leading to $|\rho| = 0.1$.⁷ Volume range of the crystals measured: $0.03 \text{ mm}^3 \leq 0.37 \text{ mm}^3$, $T = 295 \text{ K}$.*Maximum reflection coefficient, sample size and unloaded Q_0 of the cavity*

As calculations and measurements with metal spheres of different diameters have shown, the linear approximation (11) of the exact relation 9 is valid precisely, if the voltage reflection coefficient ρ is limited by the condition

$$|\rho| \leq 0.1 \quad (18)$$

On the other hand, the size of the single crystals should be as large as possible with large length/thickness ratios, R , for accuracy reasons. This latter condition leads to crystal volumes of $v_s = 0.1\text{--}0.3 \text{ mm}^3$ with $3 < R < 5$ as useful R range. However, usual Q_0 values near 1000–5000 result in reflection coefficients excessively higher than 0.1 using these crystals. Therefore, the unloaded Q_0 of the cavity had to be lowered to the values, given in Table 1, column 3. In this low- Q_0 range, the unwanted Q -lowering by the ϵ''_{eff} of the sample was about 5% (column 6, Table 1) and was neglected in the accuracy range given here. Column 8 and column 4 of this table list the crystal volume and the sphere diameter, which lead to $|\rho| \approx 0.1$ according to our basic condition, Eqn. 18. Column 5 shows the cavity detuning $\Delta\nu$ by a sphere of radius, r_M . Proportionality $\Delta\nu \sim r_M^3$ holds in the accuracy range given up to $|\rho| = 0.2$.

Experimental

Fig. 3 shows the block diagram, which is common to the three setups built here. A 100 mW reflex klystron was used as microwave source in every case. The cavities used are sketched in Fig. 4. The Q_0 of the two rectangular cavities was lowered by attaching an absorber (as shown in Fig. 5) to the small backside of the cavity by

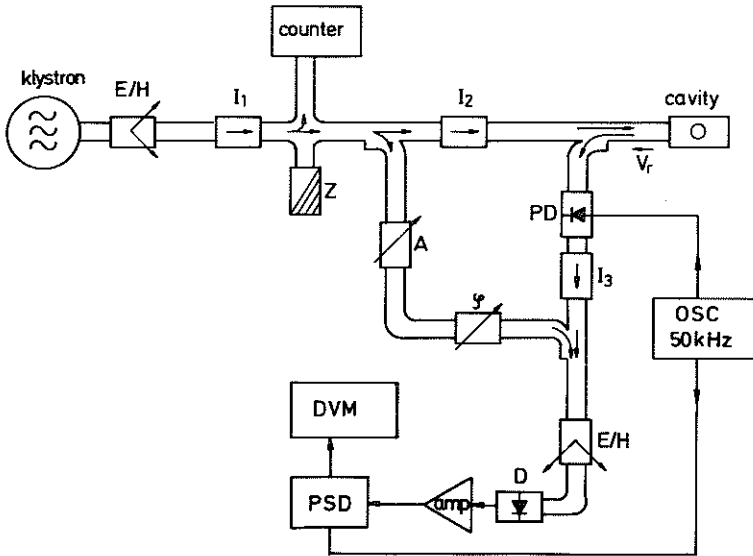


Fig. 3. Block diagram of the experimental set-up (X-band). (E/H), E-H tuner; (I_1 , I_2 , I_3), isolators; (A), variable attenuator; (ρ), variable phase shifter; (PD), pin-diode modulator; (amp), low frequency amplifier; (PSD), phase sensitive detector; (OSC), low frequency oscillator, 50 kHz; (DVM), digital voltage meter. X-band, K-band and S-band set ups are identical concerning the electronic components.

In the X-band and K-band waveguides are used, in the S-band they are replaced by semi rigid cable.

means of a coupling iris of suitable size. The resulting Q_0 values are given in Table 1, column 3. The reflected voltage, V_r , containing the information is modulated by a pin diode PD with a rectangular voltage (50 kHz). The important isolator I_3 prevents unwanted back modulations. Together with this modulated signal a large unmodulated bias reaches the detector, D . The attenuator A and the phase shifter, ρ , determine the bias amplitude and phase. This bias phase permits the discrimination between ϵ' and ϵ'' measurements as described above.

After proper choice of the phase of the microwave bias, the attenuation of A has to be adjusted in every experiment (Fig. 1A–D) precisely in such a way, that the dc-current of the detector D , which is essentially due only to the bias, remains constant. This assures, that the constant k appearing in Eqn. 1 has the same value in the measurements A–D. Three further points are of practical importance: The phase discrimination as discussed and the linearity condition inherent in Eqn. 1 both afford a high ratio of bias to signal voltage. Both conditions were fulfilled with bias dc-currents of $800 \mu\text{A}$ and signal dc-currents of about $6 \mu\text{A}$ (point contact diodes).

The overall sensitivity is determined first by the cavity Q_0 and the power levels, but practically by the mechanical guide of the sample. We give a resolution of $\Delta\epsilon'/\epsilon' \approx 1.5 \cdot 10^{-2}$ as a rough value for all set-ups, the resolution of ϵ'' being even better. The sample holder is described in Fig. 5 in detail. Since the method is based on the first-order perturbation theory and uses a well-defined reference measure-

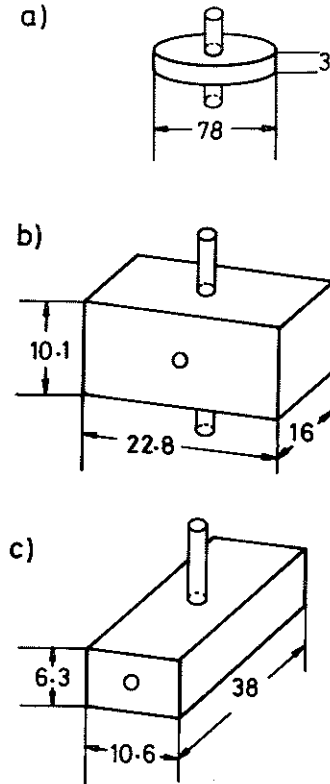


Fig. 4. Inner dimensions (in mm) of the cavities for the three frequencies (a) $\nu = 3.06$ GHz, (b) $\nu = 8.76$ GHz and (c) $\nu = 17.0$ GHz.

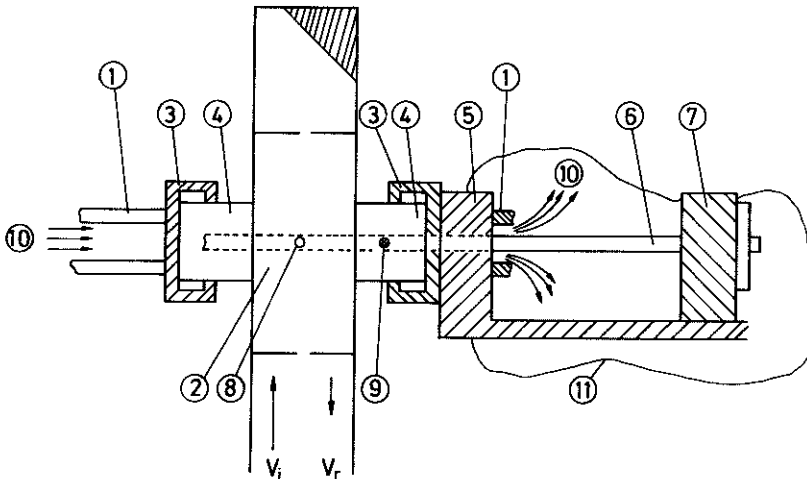


Fig. 5. Sectional drawing of the sample holder. A quartz dewar vessel (1) (outer diameter 7.6 mm, inner diameter 3.6 mm) is inserted in the cavity (2) and centered there by two Teflon rings (3). Two brass pipes (4) soldered on the cavity prevent microwave leakage. A movable support (5), (7)/(11), which holds a small closed quartz sample pipe (6) (inner diameter 2.0 mm), can be shifted in the quartz dewar so that the sample (8) or the metal sphere (9) is in the cavity centre. A thermostated N_2 -stream (10) tempers the quartz sample pipe. This sample holder is used in the K, X, and S-band.

ment, the field distribution in the cavity needs not to be known. Therefore, the same sample unit, consisting of quartz dewar (1), quartz sample pipe (6) and movable support (5)/(7) could be used in all three setups, giving high security in comparing frequency and temperature dependencies. For further details see [12].

Results

First two checks of the overall accuracy have been made:

Water measurements

Dividing Eqn. 1b by 1c gives $\epsilon''/(\epsilon' - 1)$ independent of the sample volume. A thin (approximately 1/30 mm) water film lying on the inside surface of the quartz sample pipe was investigated.

The deviations of our results from literature values are given in Table 1, column 7. These deviations for $\nu = 3, 9$ and 12 GHz are -10% , $+3\%$ and $+4\%$, respectively.

Hemoglobin single crystals

Single crystals of methemoglobin with varying size and length to thickness ratios were measured at $T = 295$ K. The results are shown in Table 1, columns 9 and 10, together with the standard deviations of the mean values. The crystal area was determined microscopically, the thickness by absorption measurements at 633 nm ($\epsilon = 4400 \text{ l} \cdot \text{mol}^{-1} \cdot \text{cm}^{-1}$) or 700 nm ($\epsilon = 178 \text{ l} \cdot \text{mol}^{-1} \cdot \text{cm}^{-1}$). The overall volume error was estimated to 8%. The relative changes of Q due to the sample (corresponding to $|\rho| = 0.1$) are given in Table 1, column 6 and are 4–6%. Errors due to residual and surface mother liquid are low with high crystal volumes and vice versa. Correspondingly, the mother liquid error could be held low (2–4%) in both ϵ' and ϵ'' measurements by careful preparation and cleaning of the crystals. That error contribution can be made smaller, if larger single crystals or sample sheets with sufficient length to thickness ratio are available. Then the cavity Q must be lowered further, to fulfill condition 18.

Application of the method: The permittivity of hemoglobin single crystals between 180 and 300 K

Fig. 6 shows the values of the complex permittivity of hemoglobin single crystals in a temperature range between 180 and 300 K. The values of ϵ' and ϵ'' are determined at three frequencies, $\nu = 3.06$ GHz, $\nu = 8.76$ GHz and $\nu = 17.0$ GHz. Between 180 and 210 K the permittivity does not depend on temperature within experimental error. Between 210 and 265 K we recognize a steep increase in ϵ' and $\epsilon'' + \sigma/(\epsilon_0\omega)$ with increasing temperature. This behaviour reflects the increasing mobility of the intermolecular water molecules and side chains on the surface of the protein when the temperature is raised. To get information about the permittivity of the intermolecular water alone a simple model is applied. The whole crystal system is treated as a suspension of water-filled spheres in a protein matrix. Using the

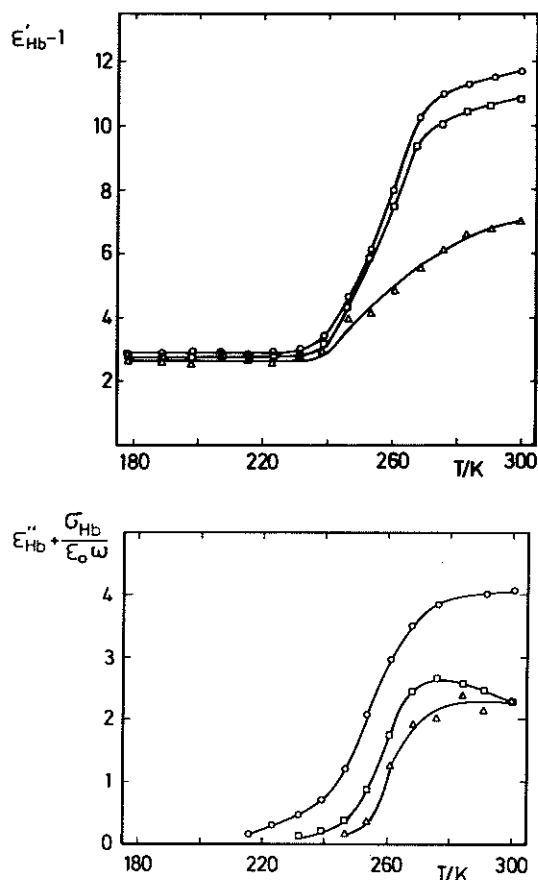


Fig. 6. The complex permittivity, $\epsilon' - 1$ (a), and $\epsilon'' = \epsilon''_{Hb} + \sigma/(\epsilon_0\omega)$ (b), of hemoglobin single crystals as a function of temperature and frequency: \circ , $\nu = 3.06$ GHz; \square , $\nu = 8.76$ GHz and Δ , $\nu = 17.0$ GHz.

known value of the water concentration, p , in a hemoglobin crystal [13], the permittivity of intermolecular water, ϵ_w^* , can be calculated from the experimental ϵ^* values. It turns out that the experimental data can be accounted for if the water spheres are composed of a core with dielectric properties of free water and a shell of water molecules with reduced rotation correlation times compared to that of free water [12]. A detailed examination of the experimental data will be given elsewhere.

Simplified description of the method and its applications

A cavity perturbation method for the absolute determination of the complex permittivity ϵ^* of small samples in the microwave range is described. The sample under test and a small reference metal sphere can be shifted alternatively into the

electric field inside a microwave cavity in a reproducible way. After the empty cavity has been tuned and matched the metal sphere is used for phase and amplitude calibrations. The definitive equations for ϵ^* of the sample do not contain amplifier and crystal characteristics, power levels and quality factors. The method may be applied to the determination of ϵ^* of samples with volumes less than 0.2 mm^3 , for example protein powder or single crystals of macromolecules. As an example the complex permittivity of methemoglobin single crystals is determined at three frequencies in a temperature range between 180 and 300 K.

References

- 1 Steinhoff, H.J. (1989) Residual motion of hemoglobin-bound spin labels as a probe for protein dynamics. *Z. Naturforsch.* 44c, 280–288.
- 2 Schauer, G., Kimmich, R. and Nusser, W. (1988) Deuteron field-cycling relaxation spectroscopy and translational water diffusion in protein hydration shells. *Biophys. J.* 53, 397–404.
- 3 Pennock, B.E. and Schwan, H.P. (1969) Further observations on the electrical properties of hemoglobin-bound water. *J. Phys. Chem.* 73, 2600–2610.
- 4 Grant, E.H., Sheppard, R.J. and South, G.P. (1978) Dielectric behaviour of biological molecules in solution. University Press, Oxford.
- 5 Thornton, J.M., Barlow, D.J. and Edwards, M.S. (1989) In: Richards, W.G. (Ed.), *Computer-Aided Molecular Design*. IBC Technical Service Ltd. London.
- 6 Ahlström, P., Telemann, O. and Jönsson, B. (1988) Molecular dynamics simulation of interfacial water structure and dynamics in a parvalbumin solution. *J. Am. Chem. Soc.* 110, 4198–4203.
- 7 Redhardt, A. and Daseler, W. (1987) A new method for absolute determination of radical concentrations by EPR. *J. Biochem. Biophys. Methods* 15, 71–84.
- 8 Sen, S., Saha, P.K. and Nag, B.R. (1979) New cavity perturbation technique for microwave measurement of dielectric constant. *Rev. Sci. Instr.* 50, 1594–1597.
- 9 Bonincontro, A. and Cametti, C. (1977) On the applicability of the cavity perturbation method to high-loss dielectrics. *J. Phys. E: Sci. Instrum.* 10, 1232–1233.
- 10 Eldumiati, I.I. and Haddad, G.I. (1972) Cavity perturbation technique for measurement of the microwave conductivity and dielectric constant of a bulk semiconductor material. *IEEE Trans. MTT* 20, 126–132.
- 11 Gobau, G. (1955) *Elektromagnetische Wellenleiter und Hohlräume*, Wiss. Verlagsgesellschaft, Stuttgart.
- 12 Daseler, W. (1987) *Eine Methode zur Messung der komplexen Dielektrizitätszahl organischer Einkristalle kleiner Abmessungen im Mikrowellenbereich*. Dissertation Ruhr-Universität Bochum, F.R.G.
- 13 Boyes-Watson, J., Davidson, E. and Perutz, M.F. (1947) An X-ray study of horse methaemoglobin I. *Proc. R. Soc.* 191 A, 83–132.